

# Cytocompatibility of Chitosan and Collagen-Chitosan Scaffolds for Tissue Engineering

Ligia L. Fernandes, Cristiane X. Resende, Débora S. Tavares, Gloria A. Soares  
Departamento de Engenharia Metalúrgica e de Materiais, UFRJ

Letícia O. Castro, Jose M. Granjeiro  
Departamento de Biologia Molecular e Celular, UFF

**Abstract:** In this work, chitosan and collagen-chitosan porous scaffolds were produced by the freeze drying method and characterized as potential skin substitutes. Their beneficial effects on soft tissues justify the choice of both collagen and chitosan. Samples were characterized using scanning electron microscope, Fourier Transform InfraRed Spectroscopy (FTIR) and thermogravimetry (TG). The *in vitro* cytocompatibility of chitosan and collagen-chitosan scaffolds was evaluated with three different assays. Phenol and titanium powder were used as positive and negative controls, respectively. Scanning electron microscopy revealed the highly interconnected porous structure of the scaffolds. The addition of collagen to chitosan increased both pore diameter and porosity of the scaffolds. Results of FTIR and TG analysis indicate that the two polymers interact yielding a miscible blend with intermediate thermal degradation properties. The reduction of XTT ((2,3-bis[2-methoxy-4-nitro-5-sulfophenyl]-2H-tetrazolium-5-carboxanilide) and the uptake of Neutral Red (NR) were not affected by the blend or by the chitosan scaffold extracts, but the blend and the titanium powder presented greater incorporation of Crystal Violet (CV) than phenol and chitosan alone. In conclusion, collagen-chitosan scaffolds produced by freeze-drying methods were cytocompatible and presented mixed properties of each component with intermediate thermal degradation properties.

**Keywords:** Collagen, chitosan, blend, cytotoxicity.

## Introduction

Patients with full thickness skin injuries and cartilage-associated diseases need biomaterials for wound healing<sup>[1]</sup>. Recently, many studies are turning towards the tissue engineering approach, whereby cells are allowed to proliferate and organize their extracellular matrix in a bi-dimensional (2-D) or three-dimensional (3-D) scaffolds. These strategies are becoming more relevant as people live for longer periods and cartilage diseases are growing fast in young people.

As a scaffold material, collagen in the form of sponges has been considered the most popular 3D scaffolds for tissue regeneration because of its excellent biocompatibility and biodegradability<sup>[1,2]</sup>. Collagen is a structural protein that has been thought to be one of the most suitable materials for constructing artificial substitutes of diseased or damaged tissues and organs<sup>[3]</sup>. However, the fast biodegradation rate and the low mechanical strength of non-crosslinked collagen scaffolds are the crucial problems that limit the further use of this material<sup>[1]</sup>. Moreover, collagen from animal source present risks of transmitting some diseases.

Chitosan is a high molar mass deacetylated product from chitin, the second most abundant polysaccharide in nature. It has structural characteristics similar to the glycosaminoglycans and exhibits numerous interesting biological properties. Additionally, the oligomers of chitosan degraded by tissue enzymes were found to be of benefit to regeneration of the skin tissue wounded areas<sup>[4]</sup>. Moreover, in contrast to the quick degradation of collagen, chitosan was found to degrade slowly *in vitro*<sup>[1]</sup>.

In the natural extracellular matrices, proteoglycans and glycosaminoglycans have important roles in intertwining with the fibrous structure of collagen to obtain mechanical stability and compressive strength<sup>[5]</sup>. Additionally, amino groups of chitosan function as binding sites with collagen to improve its stability, without significantly altering the chemical characteristics of both polymers<sup>[6]</sup>. Therefore, it may be important to develop

collagen blends with chitosan to create more suitable biomimetic microenvironments for cells.

There are many reports on collagen-chitosan scaffolds applications in tissue engineering. A variety of scaffolds have been successfully fabricated for fibroblast<sup>[1,2,7]</sup>, osteoblasts<sup>[8]</sup>, periodontal ligament cells<sup>[9]</sup>, hepatocytes<sup>[10]</sup>, lung endothelial cells<sup>[11]</sup> and to fabricate nerve guide tubes<sup>[12]</sup>. The aim of the present work is to produce a collagen-chitosan porous scaffold for tissue repair and determine its physico-chemical properties and cytocompatibility. The latter was determined by a combined parameter assay, which increases the chance of detection of cytotoxic effects, allows the correlation of different parameters and may provide hints about the mechanisms of toxicity.

## Materials and Methods

### Materials

Chitosan, with a degree of deacetylation of about 80%, was purchased from Sigma-Aldrich Co. (St. Louis, USA). Bovine type I collagen dispersion in acetic acid Apcoll-S was a gift sample from Devro Medical (Bathurst, Australia). Glacial acetic acid was purchased from VETEC Química Fina Ltda (Rio de Janeiro, Brazil). Both polymers were used as received.

### Determination of collagen concentration

Collagen concentration (2.08 mg.mL<sup>-1</sup>) was determined through its dry weight. Briefly, a glass bottle was cleaned and thoroughly dried. It was then weighed four times and the average mass was registered ( $m_b$ ). Afterwards 5 mL of the commercial collagen dispersion were added to the bottle and dried at 100 °C for one day. Once all liquid evaporated, the flask was weighed again and its final mass was registered ( $m_f$ ). Thus, collagen concentration (mg.mL<sup>-1</sup>) could be calculated as follows:

$$C_{col} = \frac{m_f - m_b}{5} \quad (1)$$

### Preparation of single component and blend scaffolds

The scaffolds used in this work were fabricated using a freeze-drying process. Briefly, a polymeric solution or suspension is allowed to freeze, inducing phase separation. During the solidification process, polymer precipitates are formed between growing ice crystals. This process produces a continuous interpenetrating network of ice and precipitates. Sublimation of the frozen solvent forms the highly porous structure of the scaffolds<sup>[13]</sup>.

Two percent (w/v) of chitosan was prepared by dissolving chitosan in 0.2 M acetic acid at room temperature. To produce the collagen-chitosan solution, the collagen dispersion (2.08 mg.mL<sup>-1</sup>) was added dropwise to the chitosan solution, while it was gently stirred. Chitosan and blend scaffolds 1:1 (w/w) were poured into 4 well cell culture dishes, frozen at -20 °C overnight and in liquid nitrogen before lyophilization for 24 hours.

### Scaffolds characterization

#### Scanning Electron Microscope (SEM)

The morphology of the scaffolds was observed using a JEOL JSM 6460 LV microscope under 20 kV. All the samples were coated with a thin gold layer using a EMITECH K550 sputter coater.

Mean pore aperture and porosity of chitosan and collagen-chitosan samples were determined by image analysis of digital SEM micrograph, using Image Pro Plus® image analysis software (Media Cybernetics). For each material, seven micrographs taken with three different magnifications (50, 100 and 150×) from different regions of three sections were used.

#### Fourier-Transformed Infra-Red Spectroscopy (FTIR)

Infra-red spectra of the prepared scaffolds were obtained in a spectrometer (Spectrum 100 PERKIN ELMER) at range of 4000 to 650 cm<sup>-1</sup>. Spectra were registered using attenuated total reflection infra-red spectroscopy (ATR-FTIR). For comparison, a collagen scaffold was also analyzed.

#### Thermal stability

Thermogravimetric and differential thermogravimetric (TG/DTG) curves were obtained in nitrogen atmosphere, using a TGA (Pyris 1 TGA PERKIN ELMER), with a heating rate of 10 °C/min, from room temperature to 700 °C. For comparison, a collagen scaffold was also analyzed.

#### Cytotoxicity test

Samples were extracted in culture medium (100 mg.mL<sup>-1</sup>, material/DMEM free of bovine fetal serum) at 37 °C for 24 hours and the extracts were collected for cytotoxicity assay according to ISO 10993-12<sup>[14]</sup> and 10993-5<sup>[15]</sup>. Phenol (1%) was used as positive control and titanium powder (100mg/ml) as negative control.

MC3T3 osteoblasts (CRL 2594 – ATCC) were seeded in 96-well cell culture plate (1 × 10<sup>4</sup>/well) and cultured in DMEM containing NaHCO<sub>3</sub> (1.2 g.L<sup>-1</sup>), ampicillin (0.025 g.L<sup>-1</sup>), streptomycin (0.1 g.L<sup>-1</sup>) supplemented with 10% bovine fetal serum for 24 hours at 37 °C under 5% CO<sub>2</sub>/95% air condition.

After 24 hours of cell exposure to each extract media, cytotoxicity was evaluated with a commercial kit (Cytotox, Xenometrix, Germany) which allows the use of 3 different parameters of cell survival and integrity on the same sample: 2,3-bis[2-methoxy-4-nitro-5-sulfophenyl]-2H-tetrazolium-5-carboxanilide (XTT), Neutral Red (NR) and Crystal Violet Dye Elution (CVDE). The XTT Cell Proliferation Assay is a colorimetric assay system

based on the ability of mitochondrial dehydrogenase enzymes to convert the yellow water-soluble tetrazolium salt XTT into orange colored soluble compounds of formazan, by their absorbance at 480 nm<sup>[16]</sup> measured with a microplate UV/Vis spectrophotometer (PowerWave MS2, BioTek Instruments, USA). NR is a survival/viability test based on the ability of living cells to incorporate the Neutral Red dye on their lysosomes, where it accumulates on membrane-intact cells<sup>[17]</sup>; the amount of dye incorporated can be measured at 540 nm. CVDE is a simple assay, which evaluates cell density by staining DNA; after elimination of the excess dye, the absorbance at 540 nm is proportional to the amount of cells in the well<sup>[18]</sup>.

All the tests were performed in quintuplicate. Mean values and standard deviations were submitted to one-way ANOVA and Tukey's post-test considering significance at 0.05.

## Results and Discussion

### Scaffold morphology

Figure 1 shows SEM micrographs of the chitosan and collagen-chitosan scaffolds. Open pore structure with a high degree of interconnectivity can be observed. Image analysis revealed that the mean pore aperture of the collagen-chitosan scaffold was around 35 µm (Figure 2b), with pores ranging from 4 to 800 µm. The mean porosity of the samples was estimated at 60%. For chitosan only, the mean pore diameter was around 16 µm and the porosity lies near 50%. Thus, it can be observed that the addition of collagen to chitosan increased both pore aperture and porosity of the scaffolds. The same trend was reported in the literature<sup>[5,6,8]</sup>. For both studied compositions a very small amount of pores with aperture larger than 300 µm was found. For a better representation, these pores were omitted in the graphs.

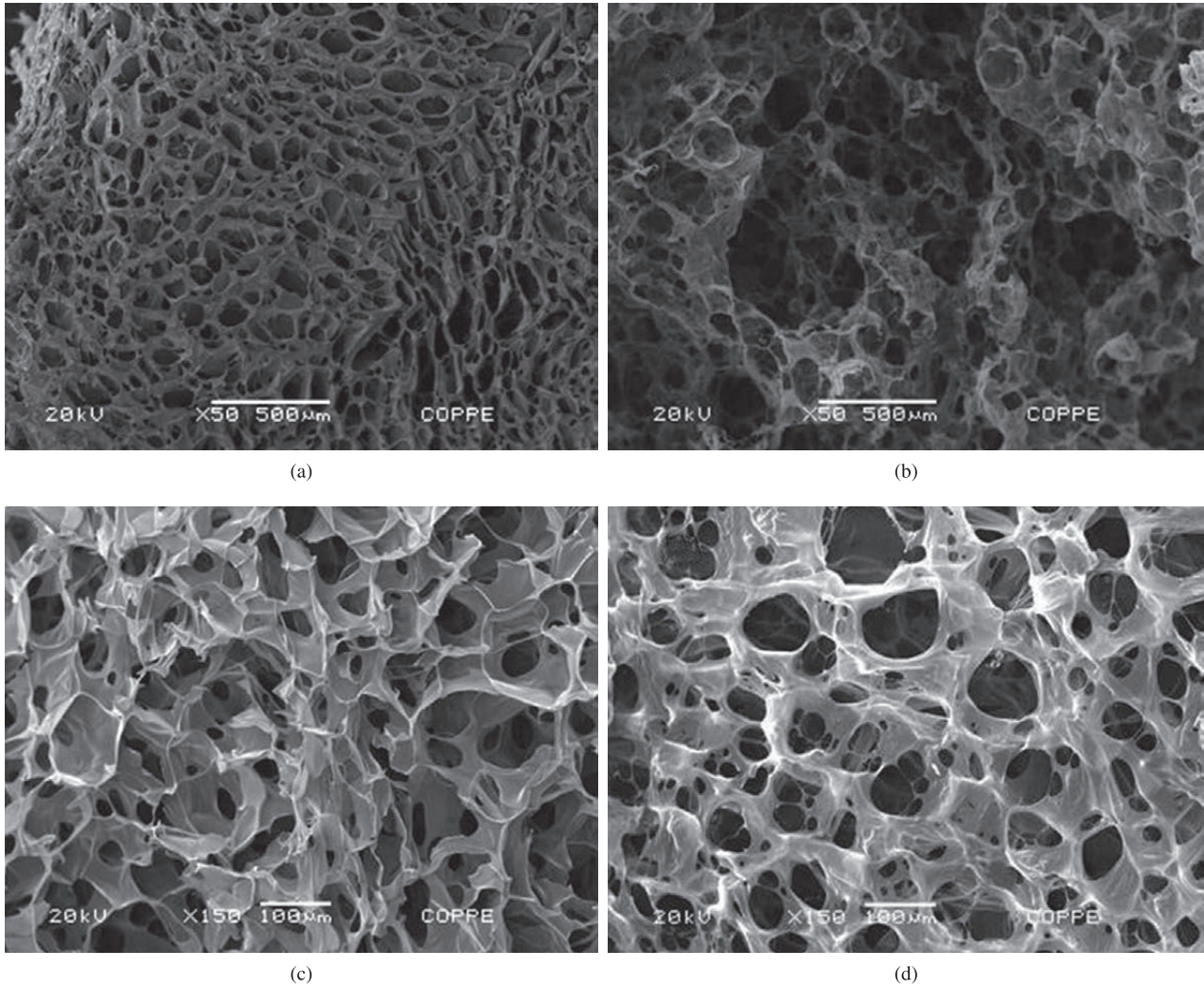
Pores size and shape were more regular for the blend scaffold. In its natural state, the collagen triple helix structure is held together by direct chemical bonds, hydrogen bonds and water bridged crosslinks<sup>[8]</sup>. The large number of amino groups in chitosan chains seems to reinforce the fibers by anchoring them in place and functions as crosslink to increase the overall matrix integrity<sup>[5,8]</sup>.

An ideal scaffold used for tissue engineering should possess the characteristic of a homogenous microstructure, suitable pore aperture and high porosity. Scaffolds must be porous to allow ingrowths of cells and migration of vascular tissue. O'Brien et al.<sup>[13]</sup> found that fibroblasts bound to a wide range of pore sizes from 63 to 150 µm and cells increased their viability with decreasing pore size until no cells could fit into the pores. Since the addition of collagen increased chitosan pore sizes, cell viability of these scaffolds might be improved.

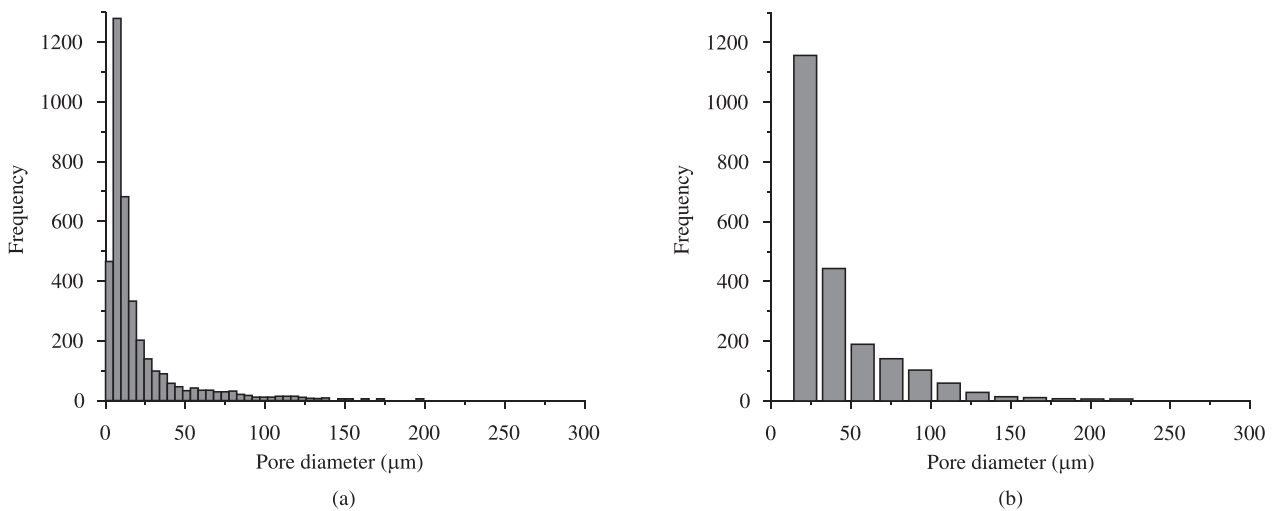
### Infrared spectroscopy

Figure 3 shows FT-IR spectra for chitosan and collagen-chitosan samples. Collagen spectrum was also obtained and included in Figure 3 in order to identify possible interactions between the two polymers in the blend samples.

The spectrum of chitosan depicts characteristic absorption bands at 3352, 2878 cm<sup>-1</sup>, attributed to the -OH and -CH<sub>3</sub> groups. Furthermore, bands were identified at 1560 and 1404 cm<sup>-1</sup> typical of the N-H group bending vibration and vibrations of -OH group of the primary alcoholic group, respectively. The bands at 1320 and 1077 cm<sup>-1</sup> correspond to the stretching of C-O-N and C-O groups. The bands at 1154 and 897 cm<sup>-1</sup> are attributed to the glycosidic bondings. The shoulder at 1650 cm<sup>-1</sup> represents the stretching of C=O. The band corresponding to free acetic acid (1706 cm<sup>-1</sup>) was not identified.



**Figure 1.** SEM micrographs a) Chitosan 50x; b) Collagen-chitosan 50x; c) Chitosan 150x; and d) Collagen-chitosan 150x.



**Figure 2.** Pore size distribution of a) chitosan; and b) collagen-chitosan scaffolds.

Collagen displayed mainly bands at 1650, 1560 and 1235  $\text{cm}^{-1}$ , characteristic of the amide I, II and III bands, respectively. The amide I absorption arises predominantly from protein amide C=O stretching vibrations and amide II is made up of amide N-H

bending vibrations and C-N stretching vibrations<sup>[19]</sup>. The amide III band is complex, consisting of components from C-N stretching and N-H in plane bending from amide linkages. It is also composed by absorptions arising from wagging vibrations from  $\text{CH}_2$  groups

from the glycine backbone and proline side-chains<sup>[19]</sup>. Additionally, bands at 3450, 2850 and 1450  $\text{cm}^{-1}$  were observed, which represent the stretching of  $-\text{OH}$ ,  $-\text{CH}_3$  and pyrrolidine rings, respectively. Once more, there was no band at 1706  $\text{cm}^{-1}$ , which suggests that there was no free acetic acid in the sample.

The FT-IR spectrum of the blend scaffolds shows the characteristic bands of the parent molecules. No additional bands were identified. The absence of new bands was confirmed through the subtraction of collagen bands from the blend scaffold spectrum, resulting in a spectrum identical to that of chitosan.

The interactions between collagen and chitosan may occur by hydrogen bonds formation. The  $-\text{OH}$ ,  $-\text{NH}_2$  and  $-\text{C}=\text{O}$  groups in collagen are capable of forming hydrogen bonds with  $-\text{OH}$  and  $-\text{NH}_2$  in chitosan<sup>[20]</sup>. Additionally, in such acidic media ( $\text{pH} < 6,5$ ), most of the amino groups of chitosan become protonated. This allows the formation of electrostatic interactions involving the  $\text{NH}_3^+$  groups of chitosan and the  $-\text{COO}^-$  groups of the aspartic and glutamic residues in collagen.

Another remarkable characteristic is that the bands corresponding to the amide I change as the level of collagen is reduced relative to the level of chitosan in a sample. As the amount of collagen in the sample decreases, the amide I band also decreases, until it is present only as a small shoulder to the amide II band, as it can be observed for the pure chitosan spectrum. On the other hand, the amide II shows a general increase as the level of chitosan is increased in the sample. The bands referring to the amide III absorption displays a loss of intensity with the increasing of the chitosan content, as previously reported<sup>[19]</sup>.

Collagen's triple helix integrity can be evaluated by the ratio between the absorbance at 1235 and at 1450  $\text{cm}^{-1}$ <sup>[21]</sup>. Ratio values for denaturated collagen are around 0.5 and those for intact structures are around 1. For the blend samples, the value obtained was 1.06, indicating that the addition of chitosan did not disestablish collagen's triple helix. This is an important feature, for this structure is considered to be responsible for collagen's biological and mechanical properties<sup>[21]</sup>.

### Thermal analysis

Thermal properties of the scaffolds were studied using thermogravimetry analysis (TG/DTG). TG curves depicting the thermal degradation behavior of the chitosan and blend scaffolds are presented in Figure 4. Data for collagen scaffolds were also included.

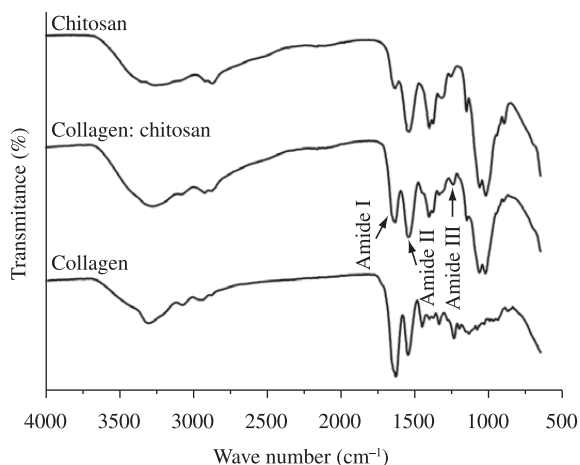


**Figure 3.** FT-IR spectra of chitosan and collagen-chitosan scaffolds. Data for collagen scaffold were also included to better characterize the blend.

The mass loss of collagen occurs in two stages: the first one is assigned to the loss of structural bound water, followed by the thermal degradation of the polymeric chains in the final stage. Chitosan and blend scaffold appears to lose mass in three different stages. The first stage refers to bound water and the second one is assigned to more strongly linked structural water<sup>[22]</sup>. The last stage refers to the degradation of the polymeric chains.

Table 1 shows peak maximum degradation temperatures obtained by differential thermogravimetry (DTG) for all scaffolds. Chitosan degradation shows a maximum at 340 °C, while for collagen it was around 400 °C. Two maximum peaks were verified for the blend scaffolds. The first one arises around 340 °C and is assigned to chitosan degradation. The other one lies in the 370 to 390 °C range, corresponding to collagen degradation, as identified by Horn et al.<sup>[22]</sup>. In comparison to the pure polymers, there is a slight change in the degradation temperature, indicating a possible interaction between them.

### Cytotoxicity test

Results of *in vitro* cytotoxicity tests for chitosan and collagen-chitosan scaffolds from XTT, NR and CVDE viability assays are given in Figure 5. XTT reduction showed that titanium (Ti, negative control) and scaffolds effects were similar to control group (cells with no extract), but phenol group was smaller than all others ( $p < 0.001$ ). No statistically significant difference was found between the biomaterials extracts and the negative control concerning the XTT reduction (Figure 5a). As expected, the positive control (1% phenol) almost impaired XTT reduction ( $p < 0.05$ ). Arpornameklong et al.<sup>[8]</sup> observed a similar trend for the same cell line.

Neutral Red stains viable cells, through the absorption of this dye, which is concentrated in its lysosomes. Neutral Red uptake was maximum for chitosan group (Figure 5b), being greater than control ( $p < 0.01$ ) and collagen-chitosan ( $p < 0.001$ ). All groups presented greater NR uptake than positive control group ( $p < 0.001$ ). Phenol impaired NR uptake ( $p < 0.001$ ).

**Table 1.** Maximum peak degradation temperature obtained by DTG.

Scaffold	Temperature (°C)
Collagen	400
Collagen:chitosan (1:1)	370-390
Chitosan	340

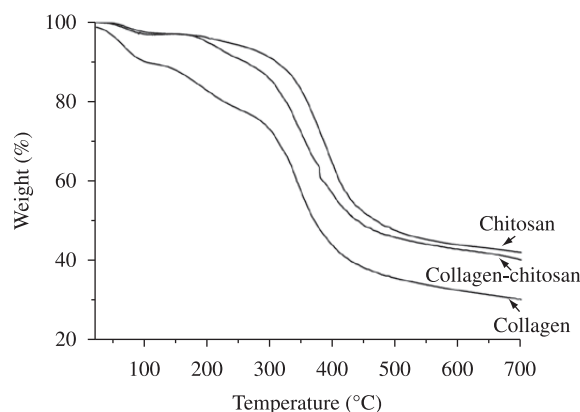


**Figure 4.** TG curves of chitosan and chitosan-collagen scaffolds. TG curve for collagen scaffold was included for comparison.

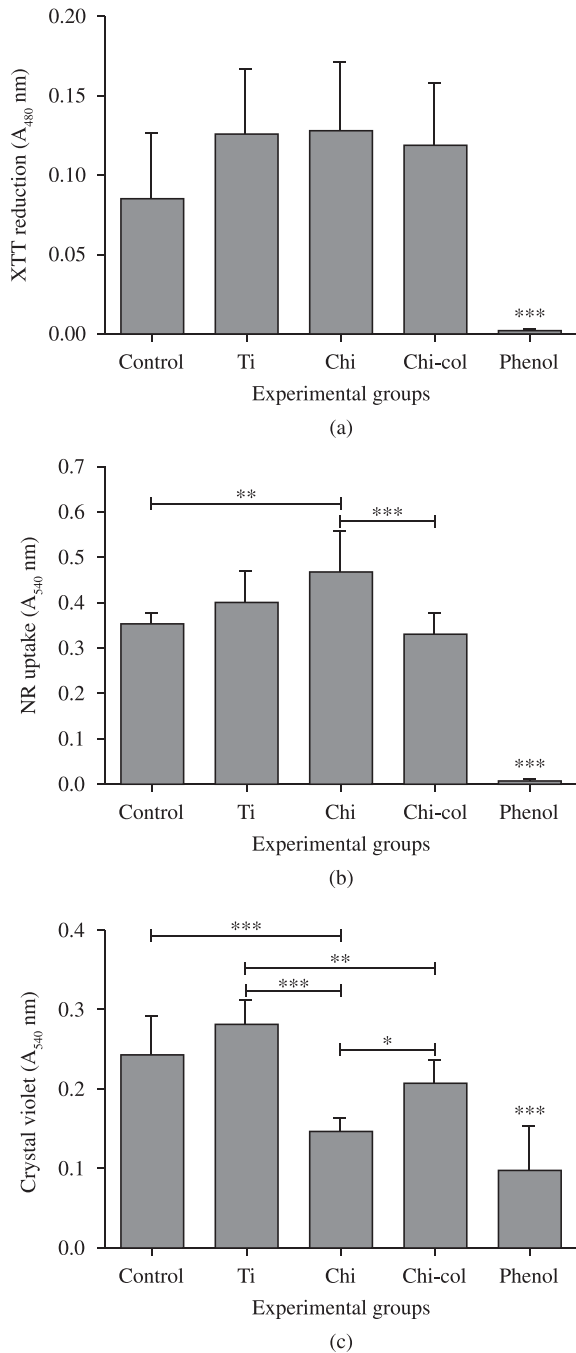


**Figure 5.** Cytotoxicity assay. Cytotoxic effects of collagen-chitosan (chi-col) and chitosan (chi) scaffolds on mouse osteoblasts. a) XTT reduction; b) Neutral Red uptake; and c) Crystal Violet Dye Elution. \*\*\*Statistically significant differences between groups ( $p < 0.001$ ). \*\* Statistically significant differences between groups ( $p < 0.01$ ). \* Statistically significant differences between groups ( $p < 0.05$ ).

Crystal violet (CV) is a dye that binds electrostatically to nuclear proteins and stains DNA. Lower amounts of CV suggested a decrease in cell number. Figure 5c indicated similar levels of CV inclusion for chitosan and phenol groups. CV DNA intercalation was lowest for chitosan and phenol groups in relation to control ( $p < 0.001$ ), negative control ( $p < 0.001$ ). The collagen association to chitosan reversed this effect, so the blend reached the same CV level of negative control.

Many assay methods are available to evaluate the cytotoxic effects of biomaterials on cultured cells. Therefore, it is important to consider more than one parameter, since residues toxicity could affect distinctly cell function<sup>[15,16,23,24]</sup>. In order to obtain a better understanding of the biomaterial toxicity, three parameters of cell viability were evaluated in parallel: lysosomal integrity and membrane permeability; dehydrogenase activity; mainly mitochondrial; and DNA content<sup>[23-25]</sup>.

Taken together, this combined cell viability assay indicates that chitosan extract alone induced cell death parallel to an increase in the lysosomal content and no effect on the mitochondria function. Nevertheless, the collagen-chitosan blend was shown to be cytocompatible.

Collagen is said to affect the cytocompatibility of chitosan<sup>[9]</sup>. First, it increases chitosan water retention ability by increasing its pore aperture. This facilitates cell attachment and penetration through the pores to form a three-dimensional growth. Second, increases the degradation of chitosan, since it collagen degrades faster *in vivo*. The degradation of collagen could help the cells penetrate inside the scaffold and cause further scaffold degradation.

## Conclusion

By using the freeze-drying method porous chitosan and collagen-chitosan scaffolds were successfully produced. The addition of collagen to chitosan increased both pore diameter and porosity of the scaffolds, measured by image analysis. Results of FTIR and TG analysis indicate that the two polymers interact yielding a miscible blend with intermediate thermal degradation properties. Collagen-chitosan scaffold was cytocompatible and tests using fibroblasts and keratinocytes are being performed to better assess its potential for skin tissue engineering. Collagen-chitosan scaffolds, produced in this work, have shown interesting properties as biomaterials.

## Acknowledgments

The authors would like to acknowledge CAPES, CNPq and FAPERJ for financial support and LABTERM EQ/UFRJ for TG analysis.

## References

1. Ma, L.; Gao, C.; Mao, Z.; Zhou, J.; Shen, J.; Hu, X. & Han, C. - *Biomaterials*, **24**, p.4833 (2003).
2. Ding, C-M.; Zhou, Y.; He, Y-N. & Tan, W-S. - *Process Biochem.*, **43**, p.287 (2008).
3. Wang, X. H.; Cui, F. Z. & Feng, Q. L. - *J. Bioact. Compat. Polym.*, **18**, p.453 (2004).
4. You, Y.; Park, W. H.; Ko, B. M. & Min, B. M. - *J. Mater. Sci.: Mater. Med.*, **15**, p.297 (2004).
5. Tan, W.; Krishnaraj, R. & Desai, T. A. - *Tissue Eng.*, **7**, p.203 (2001).
6. Zhu, Y.; Liu, T.; Song, K.; Jiang, B.; Ma, X. & Cui, Z. - *J. Mater. Sci: Mater. Med.*, **20**, p.799 (2009).
7. Wang, W.; Lin, S.; Xiao, Y.; Huang, Y.; Tan, Y.; Cai, L. & Li, X. - *Life Sci.*, **82**, p.190 (2008).
8. Arpornmaeklong, P.; Suwatwirote, N.; Pripatnanont, P. & Oungbho, K. - *Int. J. Oral Maxillofac. Surg.*, **36**, p.328 (2007).
9. Peng, L.; Cheng, X. R.; Wang, J. W.; Xu, D. X. & Wang, G. - *J. Bioact. Compat. Polym.*, **21**, p.207 (2006).
10. Wang, X. H.; Li, D. P.; Wang, W. J.; Feng, Q. L.; Cui, F. Z.; Xu, Y. X.; Song, X. H. & van der Werf, M. - *Biomaterials*, **24**, p.3213 (2003).
11. Wang, X.H.; Cui, F.Z. & Feng, Q.L. - *J Bioact. Compat. Polym.*, **18**, p.453 (2004).

12. Patel, M.; Vandevord, P. J.; Matthew, H. W.; De Silva, S.; Wu, B. & Wooley, P. H. - *J. Biomater. Appl.*, **23**, p.101 (2008).
13. O'Brien, F. J.; Harley, B. A.; Yannas, I. V. & Gibson, L. J. - *Biomaterials*, **26**, p.433(2005).
14. International Organization for Standardization. - "ISO - 10993-5. Biological evaluation of medical devices. Part 5: Tests for cytotoxicity: In vitro methods", International Organization for Standardization, Geneva (1999).
15. International Organization for Standardization. - "ISO 10993-12. Biological evaluation of medical devices. Part 12: Sample preparation and reference materials", International Organization for Standardization, Geneva (1996).
16. Scudiero, D. A.; Shoemaker, R. H.; Paul, K. D.; Monks, A.; Tierney, S.; Nofziger, T. H.; Currens, M. J.; Seniff, D. & Boyd, M. R. - *Cancer Res.*, **48**, p.4827 (1988).
17. Winckler, J. - *Prog. Histochem. Cytochem.*, **6**, p.1 (1974).
18. Kueng, W.; Silber, E. & Eppenberger, U. - *Anal Biochem.*, **182**, p.16 (1989).
19. Sionkowska, A.; Wisniewski, M.; Skopinska, J.; Kennedy, C. J. & Wess, T. J. - *Biomaterials*, **25**, p.795 (2004).
20. Chen, Z.; Mo, X.; He, C. & Wang, H. - *Carbohydr. Polym.*, **72**, p.410 (2008).
21. Tohni, E. & Plepis, A. M. G. - *Quim. Nova*, **25**, p.943 (2002).
22. Horn, M. M.; Martins, V. C. A. & Plepis, A. M. G. - *Carbohydr. Polym.*, **77**, p.239 (2009).
23. Ishiyama, M.; Tominaga, H.; Shiga, M.; Sasamoto, K.; Okhura, Y. & Ueno, K. - *Biol. Pharm. Bull.*, **19**, p.1518 (1996).
24. Takamori, E. R.; Figueira, E. A.; Taga, R.; Sogayar, M. C. & Granjeiro, J. M. - *Braz. Dent. J.*, **18**, p.179 (2007).
25. DeDeus, G.; Canabarro, A.; Alves, G.; Linhares, A.; Senne, M. I. & Granjeiro, J. M. - *J. Endod.*, **35**, p.1387 (2009).

*Enviado: 07/01/10*

*Reenviado: 01/03/10*

*Aceito: 04/03/10*

DOI: 10.1590/S0104-1428201100500008